


Hadron Energy Reconstruction for ATLAS Barrel Combined Calorimeter Using Non-parametrical Method

Yuri Kulchitsky

(for ATLAS TILECAL Collaboration)

13 October 2000

IX International Conference on Calorimetry in Particle Physics

9 – 14 October 2000, Annecy, France


Introduction

- **In this talk we describe the non-parametrical method of the energy reconstruction for a combined calorimeter, which called the e/h method, and demonstrate its performance on the basis of the test beam data of the ATLAS combined calorimeter.**
- **The aim of the present talk is also to develop the method and to determine the value of the e/h ratio of the electromagnetic compartment of combined calorimeter.**
- **This talk is also devoted to the study of the longitudinal hadronic shower development in the ATLAS barrel combined prototype calorimeter.**

ATLAS Calorimetry

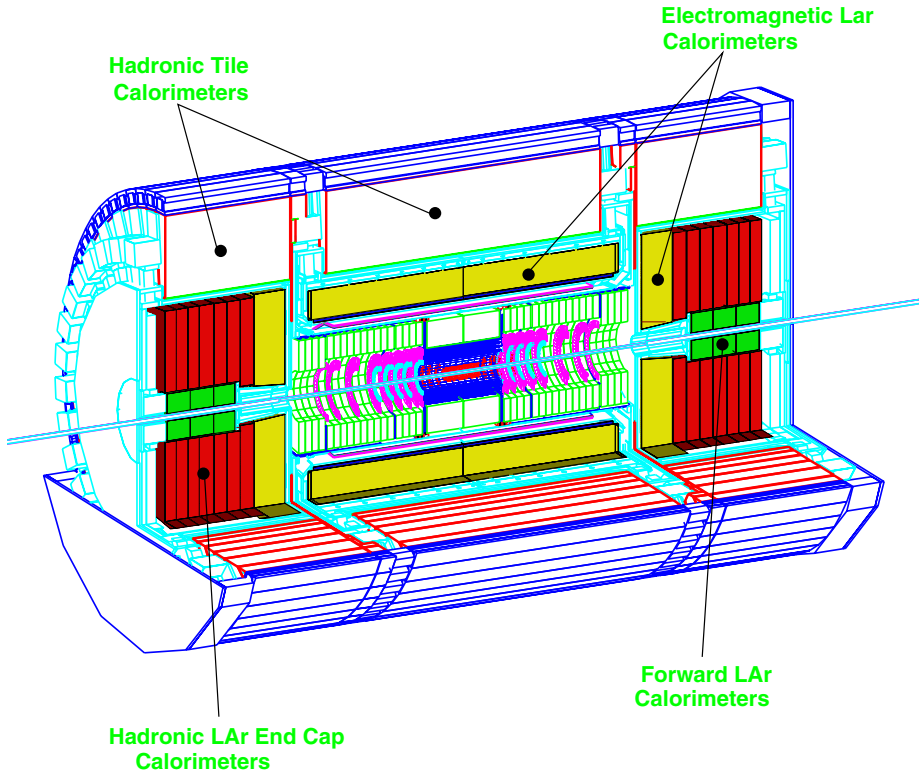

Figure 1: Three-dimensional cutaway view of the ATLAS calorimeters.


Combined Calorimeter

The Combined Calorimeter prototype setup has been made consisting of the LAr electromagnetic calorimeter prototype inside the cryostat and downstream the Tile calorimeter prototype as shown in Figure 2. The two calorimeters have been placed with their central axes at an angle to the beam of 12°. At this angle the two calorimeters have an active thickness of 10.3 λ_I.

Beam quality and geometry were monitored with a set of beam wire chambers BC1, BC2, BC3 and trigger hodoscopes placed upstream of the LAr cryostat. To detect punchthrough particles and to measure the effect of longitudinal leakage a "muon wall" consisting of 10 scintillator counters (each 2 cm thick) was located behind the calorimeters at a distance of about 1 metre.

Combined Calorimeter Setup

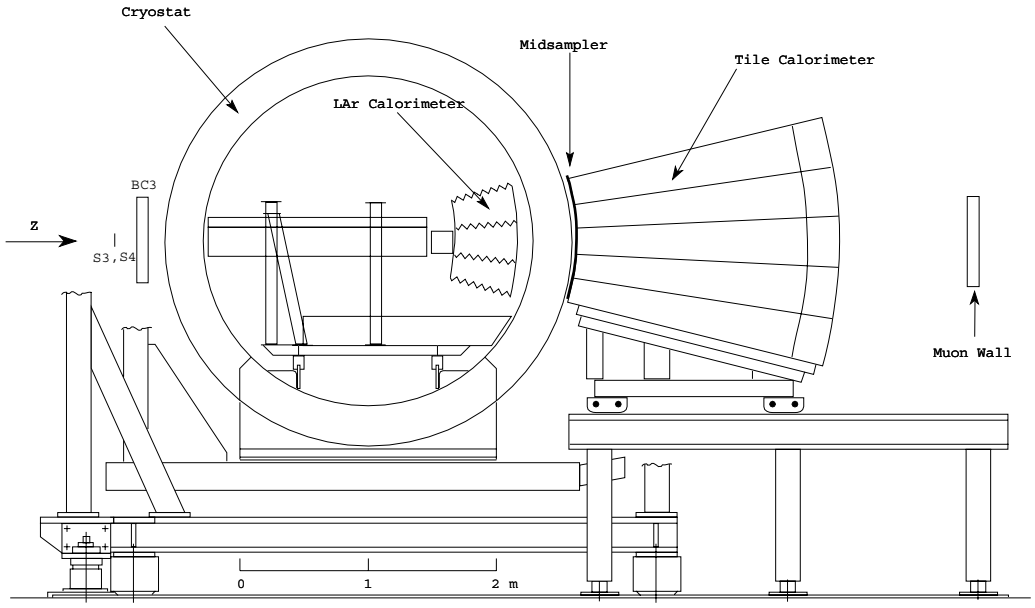

Figure 2: Schematic layout of the experimental setup for the combined LAr and Tile calorimeters run (side view). The S3 and S4 are scintillation counters, the BC3 is a beam proportional chamber, and the midsampler and the "muon wall" are scintillation hodoscopes.


Electromagnetic Calorimeter

The electromagnetic LAr calorimeter prototype consists of a stack of three azimuthal modules, each one spanning 9° in azimuth and extending over 2 m along the Z direction. The calorimeter structure is defined by 2.2 mm thick steel-plated lead absorbers folded to an accordion shape and separated by 3.8 mm gaps filled with liquid argon. The signals are collected by Kapton electrodes located in the gaps. The calorimeter extends from an inner radius of 131.5 cm to an outer radius of 182.6 cm, representing (at $\eta = 0$) a total of 25 radiation lengths (X_0), or 1.22 interaction lengths (λ_I) for protons. The calorimeter is longitudinally segmented into three compartments of 9 X_0, 9 X_0 and 7 X_0, respectively.


Cryostat

The cryostat has a cylindrical form with 2 m internal diameter, filled with liquid argon, and is made out of a 8 mm thick inner stainless-steel vessel, isolated by 30 cm of low-density foam (Rohacell), itself protected by a 1.2 mm thick aluminum outer wall.


Hadronic Calorimeter

The hadronic Tile calorimeter is a sampling device using steel as the absorber and scintillating tiles as the active material. The innovative feature of the design is the orientation of the tiles which are placed in planes perpendicular to the Z direction (Figure 3). For a better sampling homogeneity the 3 mm thick scintillators are staggered in the radial direction. The tiles are separated along Z by 14 mm of steel, giving a steel/scintillator volume ratio of 4.7. Wavelength shifting fibres (WLS) running radially collect light from the tiles at both of their open edges. The hadron calorimeter prototype consists of an azimuthal stack of five modules. Each module covers $2\pi/64$ in azimuth and extends 1 m along the Z direction, such that the front face covers 100×20 cm^2. The radial depth, from an inner radius of 200 cm to an outer radius of 380 cm, accounts for 8.9 λ at $\eta = 0$ (80.5 X_0).


Hadronic Calorimeter *(continued)*

Read-out cells are defined by grouping together a bundle of fibres into one photomultiplier (PMT). Each of the 100 cells is read out by two PMTs and is fully projective in azimuth (with $\Delta\phi = 2\pi/64 \approx 0.1$), while the segmentation along the Z axis is made by grouping fibres into read-out cells spanning $\Delta Z = 20$ cm ($\Delta\eta \approx 0.1$) and is therefore not projective. Each module is read out in four longitudinal segments (corresponding to about 1.5, 2, 2.5 and 3 λ_I at $\eta = 0$).

Tile Calorimeter

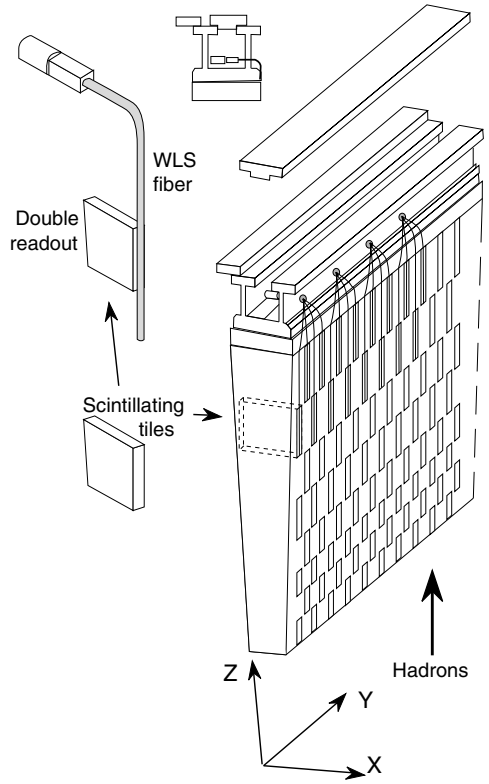

Figure 3: Conceptual design of a Tile calorimeter module.


Data Selection

This work has been performed on the basis of the 1996 ATLAS Barrel Prototype Combined Calorimeter test beam data. The data have been taken in the H8 beam line of the CERN SPS using pions of 10, 20, 40, 50, 80, 100, 150 and 300 GeV.

We applied some cuts to eliminate

- the non-single track pion events,
- the beam halo,
- the events with an interaction before the LAr calorimeter,
- the electron and muon events.

e/h Method of Energy Reconstruction

An hadronic shower in a calorimeter can be seen as an overlap of a pure electromagnetic and a pure hadronic component. The calorimeter response, R, to these two components is usually different and can be written as:

$$R = e \cdot E_e + h \cdot E_h \ , \tag{1}$$

where e (h) is a coefficient to rescale the electromagnetic (hadronic) energy content to the calorimeter response. From this:

$$E = (1/e) \cdot (e/\pi) \cdot R \ , \tag{2}$$

$$\frac{e}{\pi} = \frac{e/h}{1 + (e/h - 1) \cdot f_{\pi^0}} \ , \tag{3}$$

$$f_{\pi^0} = E_e/E = k \cdot \ln E \ . \tag{4}$$

e/h **Method** *(continued)*

In the case of the combined setup, the total energy is reconstructed as the sum of the energy deposit in the electromagnetic compartment (E_{LAr}), the deposit in the hadronic calorimeter (E_{Tile}), and that in the passive material between the LAr and Tile calorimeters (E_{dm}).

Expression (2) can then be rewritten as:

$$E = E_{LAr} + E_{dm} + E_{Tile} = \left\{ \frac{1}{e}\left(\frac{e}{\pi}\right) R \right\}_{LAr} + E_{dm} + \left\{ \frac{1}{e}\left(\frac{e}{\pi}\right) R \right\}_{Tile}, \quad (5)$$

where R_{LAr} (R_{Tile}) is the measured response of the LAr (Tile) calorimeter compartment and $1/e_{Tile}$ and $1/e_{LAr}$ are energy calibration constants for the LAr and Tile calorimeters respectively.

E_{dm}

Similarly to the procedure in Reference *("Results from an Expanded Combined Test of the Electromagnetic Liquid Argon Calorimeter with a Hadronic Scintillating-Tile Calorimeter", NIM* **A499***, 2000, 461)* the E_{dm} term, which accounts for the energy loss in the dead material between the LAr and Tile calorimeters, is taken to be proportional to the geometrical mean of the energy released in the third depth of the electromagnetic compartment and the first depth of the hadronic compartment

$$E_{dm} = \alpha \cdot \sqrt{E_{LAr,3} \cdot E_{Tile,1}} \ . \qquad (6)$$

The validity of this approximation has been tested using a Monte Carlo simulation along with a study of the correlation between the energy released in the midsampler and the E_{dm}.


$1/e_{Tile}$ and $1/e_{LAr}$

The ratio $(e/h)_{Tile} = 1.3 \pm 0.03$ has been measured in a stand-alone test beam run and is used to determine the $(e/\pi)_{Tile}$ term in equation 5. To determine the value of the $1/e_{Tile}$ constant we selected events which started showering only in the hadronic compartment, requiring that the energy deposited in each sampling of the LAr calorimeter and in the midsampler is compatible with that of a single minimum ionization particle. $1/e_{Tile}$ is then defined

$$1/e_{Tile} = \frac{E_{beam}}{< R_{Tile} > \cdot (e/\pi)_{Tile}} = 0.145 \pm 0.002 \qquad (7)$$

with this numerical value obtained by taking the average of all the beam energies available.

The response of the LAr calorimeter has already been calibrated to the electromagnetic scale; thus the constant $1/e_{LAr} = 1$


e/h of the Electromagnetic Compartment

Using the expression (5) the value of the $(e/\pi)_{LAr}$ ratio can be obtained

$$\left(\frac{e}{\pi}\right)_{LAr} = \frac{E - E_{dm} - E_{Tile}}{c_{LAr} \cdot R_{LAr}} \ . \qquad (8)$$

The $(e/h)_{LAr}$ ratio and the function $f_{\pi^0,LAr}$ can be inferred from the energy dependent $(e/\pi)_{LAr}$ ratios. For this case we select the events with the well developed hadronic showers in the electromagnetic calorimeter. Than mean that energy depositions were required to be more than 10% of the beam energy in the electromagnetic calorimeter and less than 70% in the hadronic calorimeter. Figure 4 shows the distributions of the $(e/\pi)_{LAr}$ ratio derived by formula (8) for different energies.

e/π

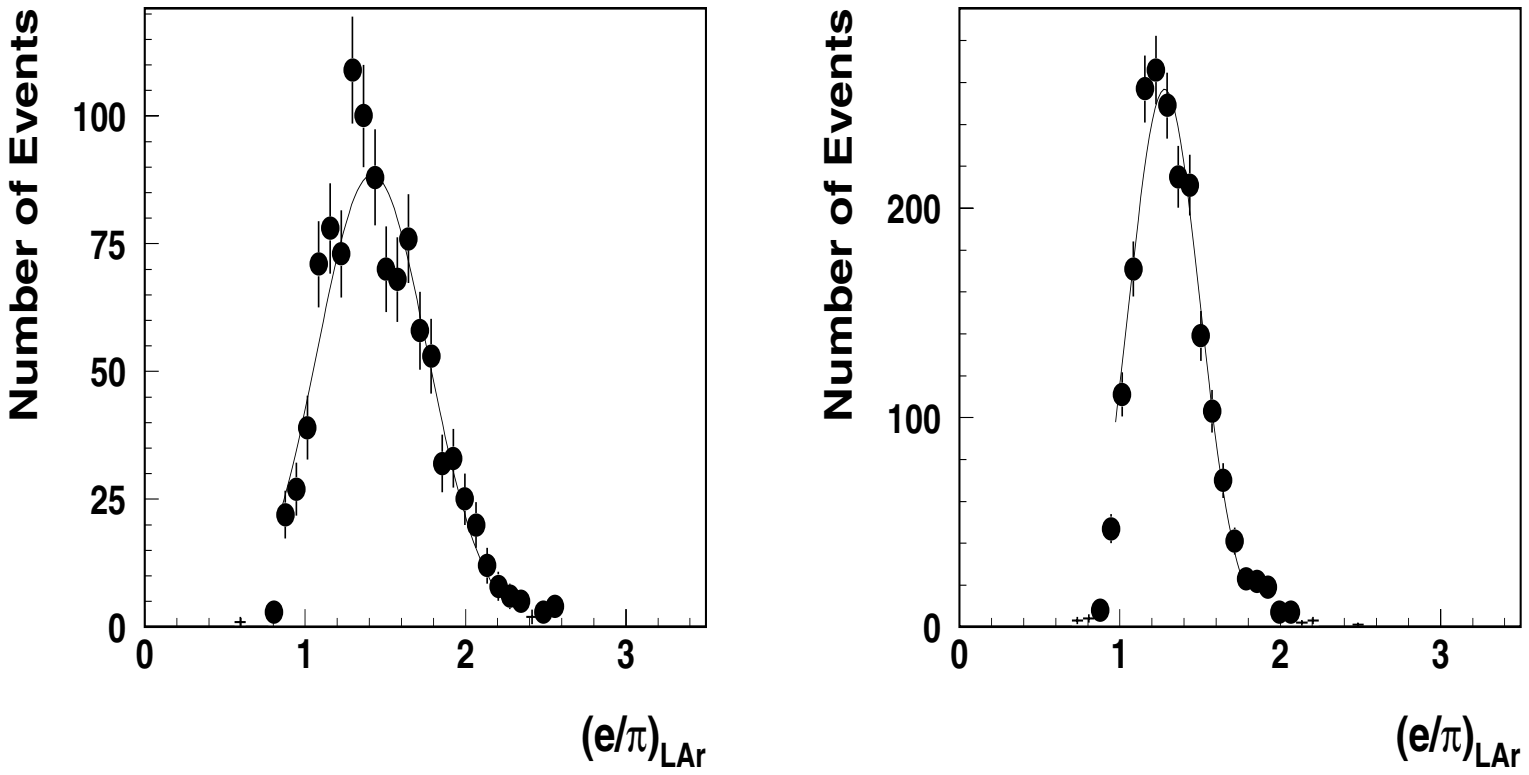

Figure 4: The distributions of the $(e/\pi)_{LAr}$ ratio for $E_{beam} = 20$ (left) and 100 (right) GeV.


e/h of the LAr *(continued)*

The mean values of these distributions are shown in Figire 5 as a function of the beam energy. The fit of this distribution by the expression (3) for LAr calorimeter yields

$$(e/h)_{LAr} = 1.74 \pm 0.04 \; and \; k = 0.108 \pm 0.004 \; (\chi^2/NDF = 0.93).$$

For the fixed value of the parameter $k = 0.11$ *(R. Wigmans, Proc. 2nd Int. Conf. on Calorimetry in HEP, Capri, 1991)* the result is

$$(e/h)_{LAr} = 1.77 \pm 0.02 \;\; (\chi^2/NDF = 0.86).$$

The quoted errors are the statistical ones obtained from the fit. The systematic error on the $(e/h)_{LAr}$ ratio, which is a consequence of the uncertainties in the input constants used in the equation (8), is estimated to be ± 0.04.

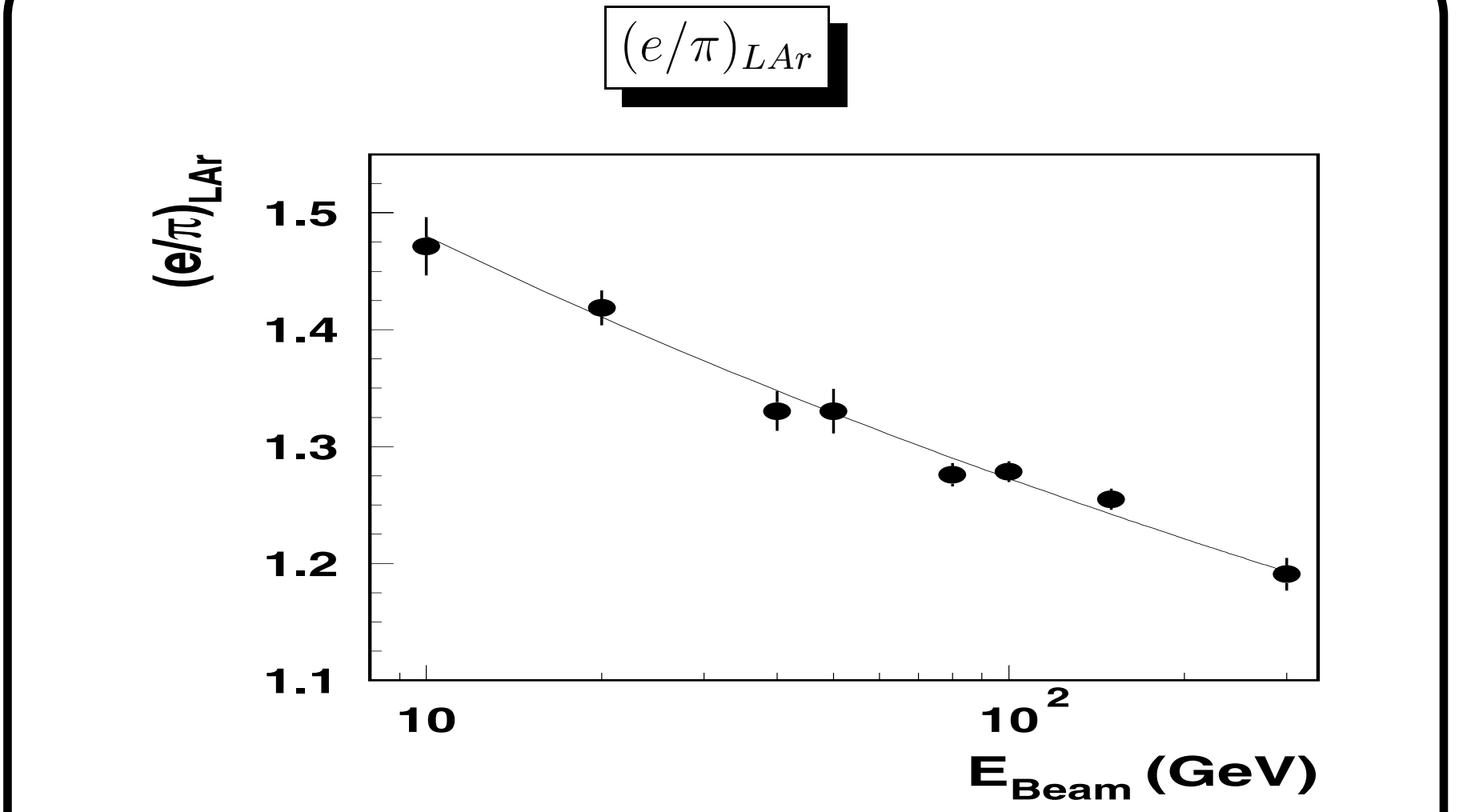

Figure 5: The mean value of the $(e/\pi)_{LAr}$ ratio as a function of the beam energy.


Comparison with Monte Carlo

Wigmans showed that the e/h ratio for non-uranium calorimeters with high-Z absorber material is satisfactorily described by the formula:

$$\frac{e}{h} = \frac{e/mip}{0.41 + f_n \cdot n/mip} \ , \tag{9}$$

where f_n is a constant determined by the Z of the absorber (for lead $f_n = 0.12$) and e/mip and n/mip represent the calorimeter response to e.m. showers and to MeV-type neutrons, respectively. These responses are normalized to the one for minimum ionizing particles. The Monte Carlo calculated e/mip and n/mip values for the R&D3 Pb-LAr electromagnetic calorimeter are $e/mip = 0.78$ and $n/mip < 0.5$ leading to

$$(e/h)_{LAr} > 1.66.$$


Comparison with Monte Carlo *(continued)*

Formula (9) indicates that e/mip is very important for understanding compensation in LAr calorimeters. The degree of non-compensation increases when the sampling frequency is also increased. A large fraction of the electromagnetic energy is deposited through very soft electrons ($E < 1$ MeV) produced by Compton scattering or the photoelectric effect. The cross sections for these processes strongly depend on Z and practically all these photon conversions occur in the absorber material. The range of the electrons produced in these processes is very short, ~ 0.7 mm for 1 MeV electron in lead. Such electrons only contribute to the calorimeter signal if they are produced near the boundary between the lead and the active material.


Comparison with Monte Carlo *(continued)*

The Monte Carlo calculations also predict that the electromagnetic response for liquid-argon calorimeters (due to the larger Z value of Argon) is consistently larger than for calorimeters with plastic-scintillator readout. The signal from neutrons (n/mip) is suppressed by a factor 0.12 and the $n-p$ elastic scattering products do not contribute to the signal of liquid-argon calorimeters. These detectors only observe the γ's produced by inelastic neutron scattering and from thermal neutron capture.


Comparison with Weiting Method

In the *(M.Stipcevic, "First Evaluation of Weighting Techniques to Improve Pion Energy Resolution in Accordion Liquid Argon Calorimeter", CERN-RD3-Note-44, 1993)* and *(D.M.Gingrich et al., NIM* **A355**, *1995, 290)* the following definition of an e/π ratio for first compartment (LAr) of the combined calorimeter is adopted. The estimators for pion and electron energies, respectively, are

$$E = c^{\pi}_{em} \cdot R_{em} + c^{\pi}_{had} \cdot R_{had} \ ,$$

$$E = c^{e}_{em} \cdot R_{em} \ ,$$

where R_{em} and R_{had} are responses of elecromagnetic and hadronic compartments of a combined calorimeter, c^{e}_{em} (energy independent within 1%) is the energy calibration constant for the electromagnetic calorimeter, c^{π}_{em} and c^{π}_{had} are weighting parameters for pions.

Comparison with Weiting Method *(continued)*

These parameters was find using a minimisation procedure for a energy resolution (σ/E) at every beam energies. An electron/pion ration defined as

$$(e/\pi)_{em} = c^{\pi}_{em}/c^{e}_{em} \ .$$

This definition one can find from (5) for an electromagnetic compartment, where

$$c^{\pi}_{em} = 1/e_{em} \cdot (e/\pi)_{em} \ , \qquad 1/e_{em} = c^{e}_{em} \ .$$

The results of this weighting method for $(e/\pi)_{em}$ rations present on the Figures 6. In the energy region ≤ 100 GeV the our data are in a good agreement with RD3 data and in disagreement for energies > 100 GeV.

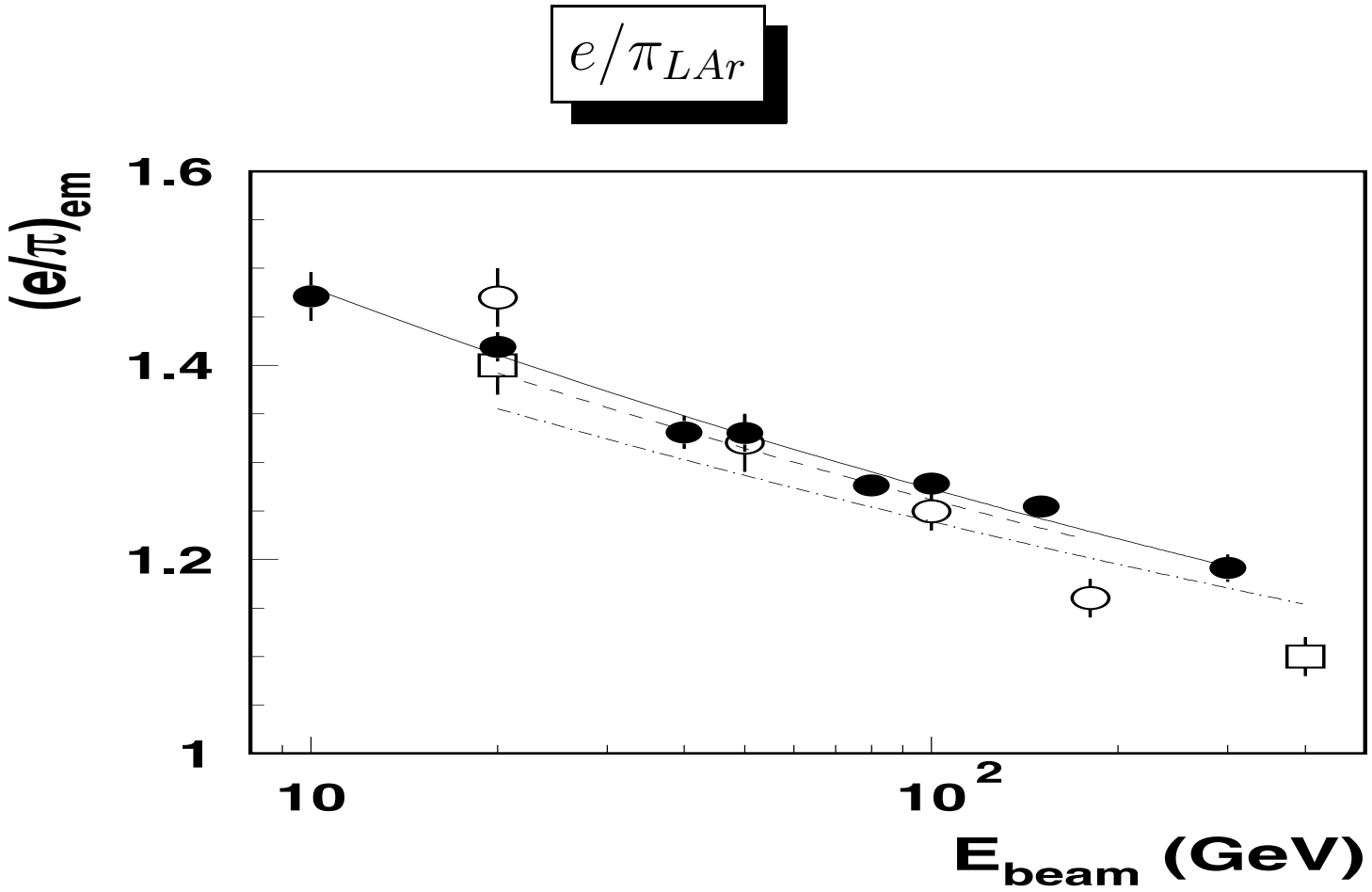

Figure 6: The $(e/\pi)_{em}$ ratios as a function of the beam energy for this method (black circles) and for weighting method (open circles for *Stipcevic* and open squares for *Gingrich*).

Comparison with Weiting Method *(continued)*

Fit of the $(e/\pi)_{em}$ values by the expression (3), with two parameters, yields

$$(e/h)_{em} = 2.28 \pm 0.19 \; and \; k = 0.143 \pm 0.006 \; (Stipcevic)$$

$$(e/h)_{em} = 1.93 \pm 0.13 \; and \; k = 0.135 \pm 0.007 \; (Gingrich)$$

Note, that problematical value of $(e/\pi)_{em} = 0.96 \pm 0.02$ at 300 GeV is excluded from the fit. One can see that parameters k are more bigger that its well known value and the $(e/h)_{em}$ are bigger than our result. For fixed parameter $k = 0.11$ the result of the fit are

$$(e/h)_{em} = 1.73 \pm 0.10 \; and \; (e/h)_{em} = 1.64 \pm 0.18 \; .$$

The weighting method leads to distortion of the $(e/\pi)_{em}$ ratios.

Iteration Procedure

For the energy reconstruction by the formula (5) it is necessary to know the $(e/\pi)_{Tile}$ ratio and the reconstructed energy itself. Therefore, the iteration procedure has been developed. Two iteration cycles were made: the first one is devoted to the determination of the $(e/\pi)_{Tile}$ ratio and the second one is the energy reconstruction itself. The expression (3) for the $(e/\pi)_{Tile}$ ratio can be written as

$$\left(\frac{e}{\pi}\right)_{Tile} = \frac{(e/h)_{Tile}}{1 + ((e/h)_{Tile} - 1) \cdot k \cdot \ln\left(c_{Tile} \cdot (e/\pi)_{Tile} \cdot R_{Tile}\right)} \ . \quad (10)$$

As the first approximation, the value of $(e/\pi)_{Tile}$ is calculated using the equation (10) where in the right side of this equation we used $(e/\pi)_{Tile} = 1.13$ corresponding to $f_{\pi^0,Tile} = 0.5$.


Iteration Procedure

The iteration process is stopped when the convergence criterion

$$| (e/\pi)^{\nu+1}_{Tile} - (e/\pi)^{\nu}_{Tile} | /(e/\pi)^{\nu}_{Tile} < \epsilon \ ,$$

where ($\nu = 0,\ 1, \ldots$), is satisfied. As the first approximation in the iteration cycle for the energy reconstruction, the value of E is calculated using the equation (5) with the $(e/\pi)_{Tile}$ ratio obtained in the first iteration cycle and $(e/\pi)_{LAr}$ from equation (3) where in the right side of this equation we used $(e/\pi)_{LAr} = 1.27$ corresponding to $f_{\pi^0,LAr} = 0.5 = 0.11 \ln(100\ GeV)$. The average numbers of iterations $< N_{it} >$ for the various beam energies needed to receive the given value of accuracy ϵ have been investigated (Figures 7 and 8). It turned out, it is sufficiently only the first approximation for achievement, on average, of convergence with an accuracy of $\epsilon = 1\%$.

Linearity

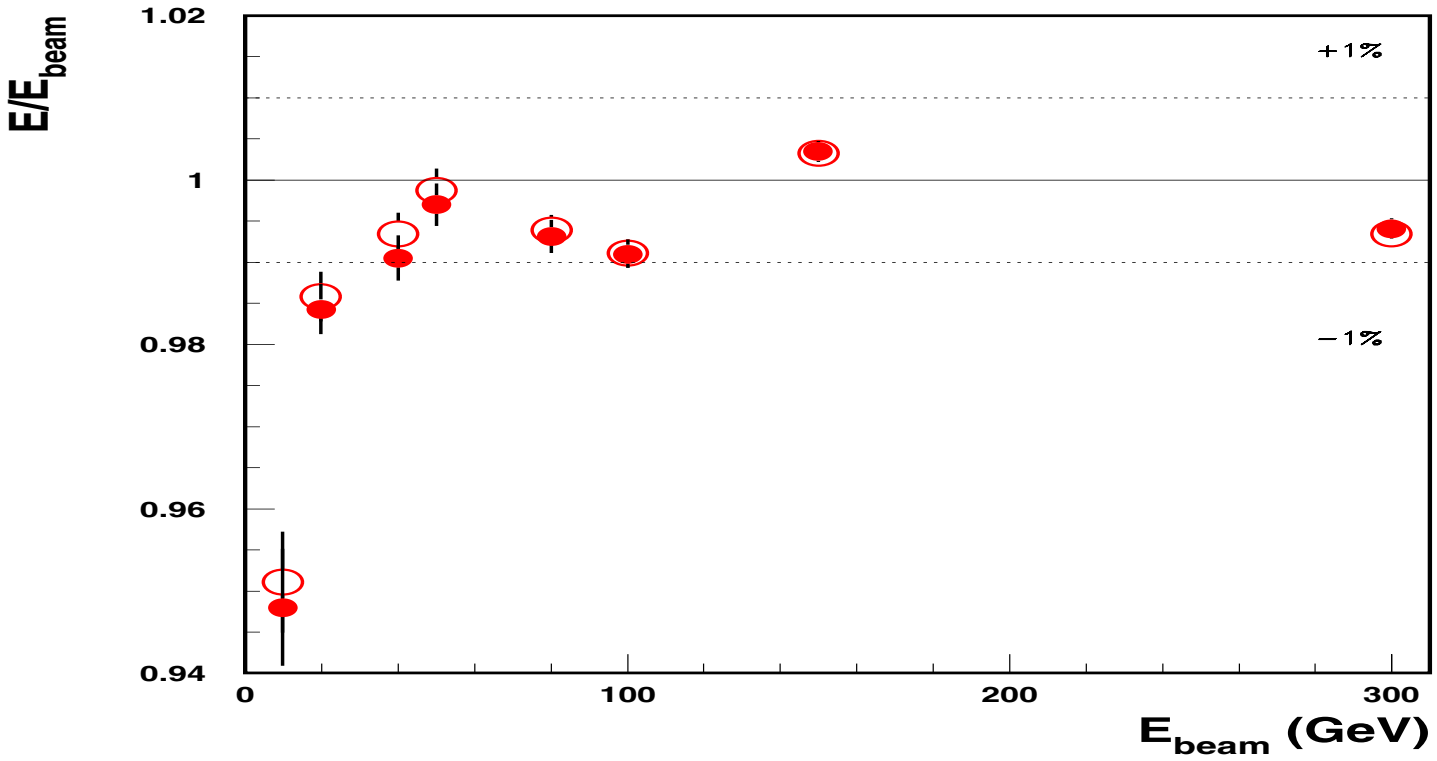

Figure 7: Energy linearity as a function of the beam energy for the e/h method obtained using the iteration procedure with $\epsilon = 0.1\%$ (black circles) and the first approximation (open circles).

Resolution

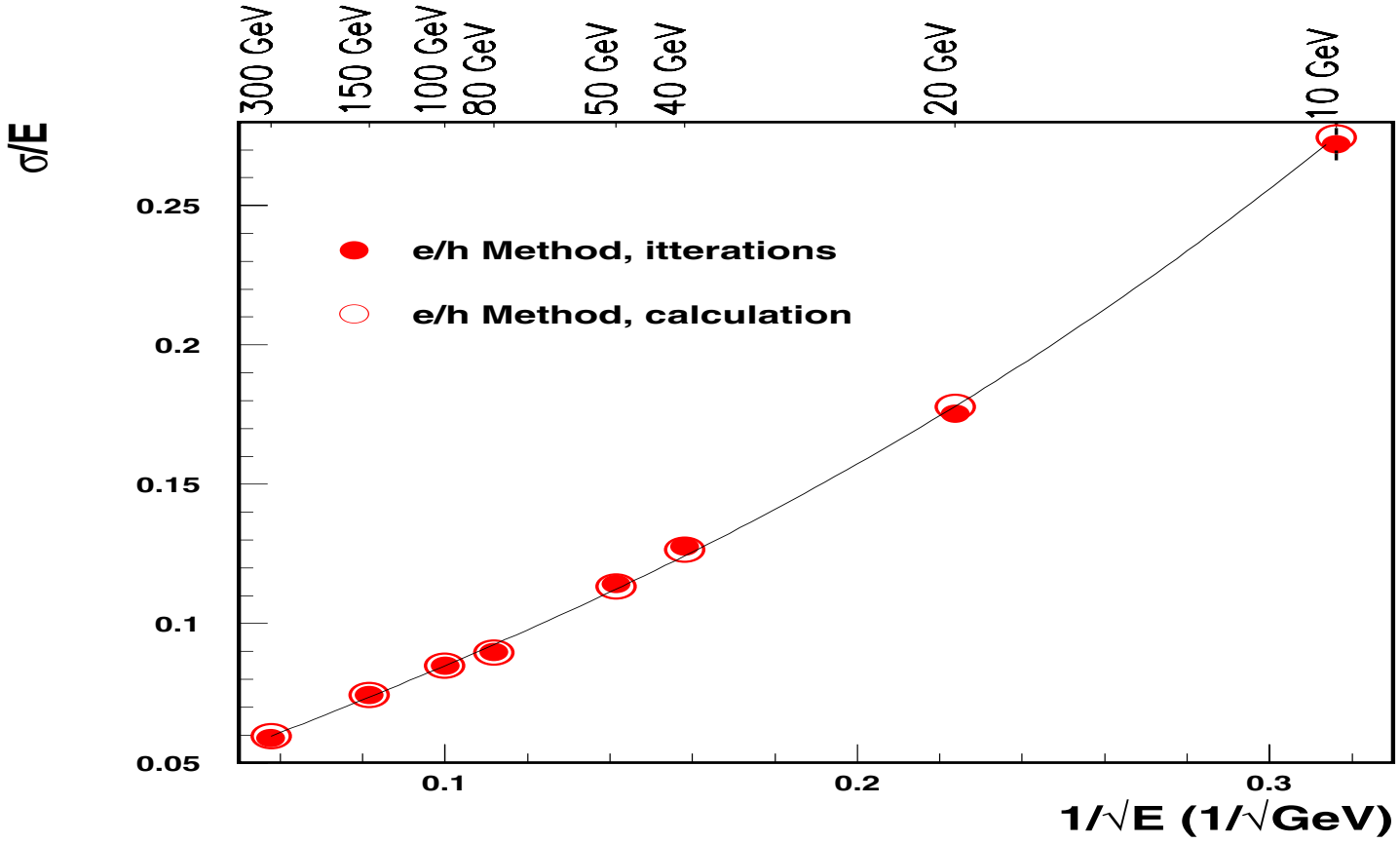

Figure 8: The fractional energy resolutions obtained with the $\epsilon = 0.1\%$ (black circles) and the first approximation (open circles).


Energy Spectra

Figure 9 shows the pion energy spectra reconstructed with the e/h method ($\epsilon = 0.1\%$).

The mean and σ values of these distributions are extracted with Gaussian fits over $\pm 2\sigma$ range.

Energy

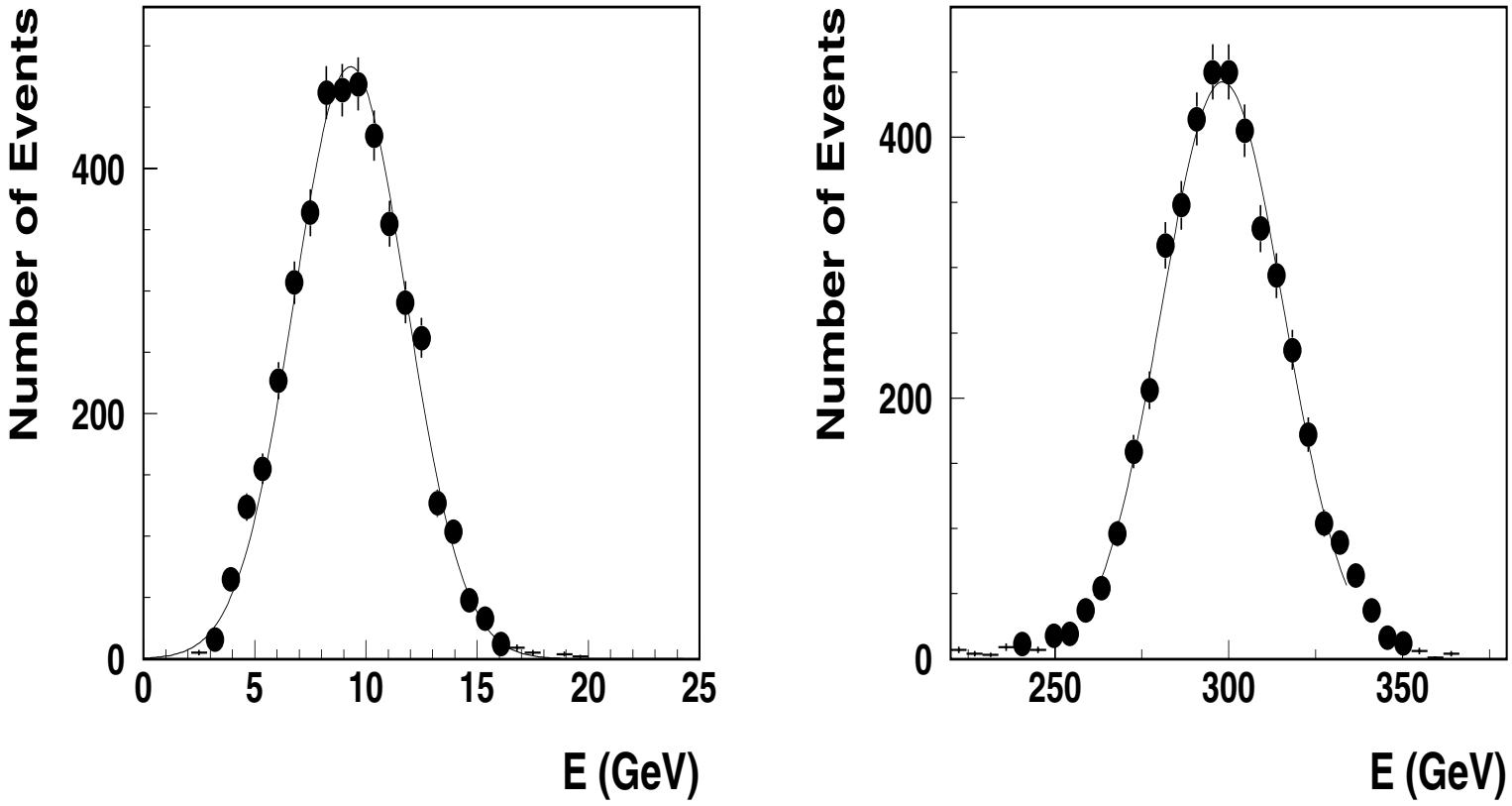

Figure 9: The energy distributions for $E_{beam} = 10$ (left) and 300 (right) GeV.


Energy Linearity

Figure 10 demonstrates the correctness of the mean energy reconstruction. The mean value of E/E_{beam} is equal to $(99.5 \pm 0.3)\%$ and the spread is $\pm 1\%$ except for the point at 10 GeV. But at this point the result is strongly dependent on the effective capability to remove events with interactions in the dead material upstream and to deconvolve the real pion contribution from the muon contamination.

Figure 10 also shows the comparison of the linearity, E/E_{beam}, as a function of the beam energy for the e/h method and for the cells weighting method. As can be seen, the comparable quality of the linearity is observed for these two methods.

Linearity: e/h and CW

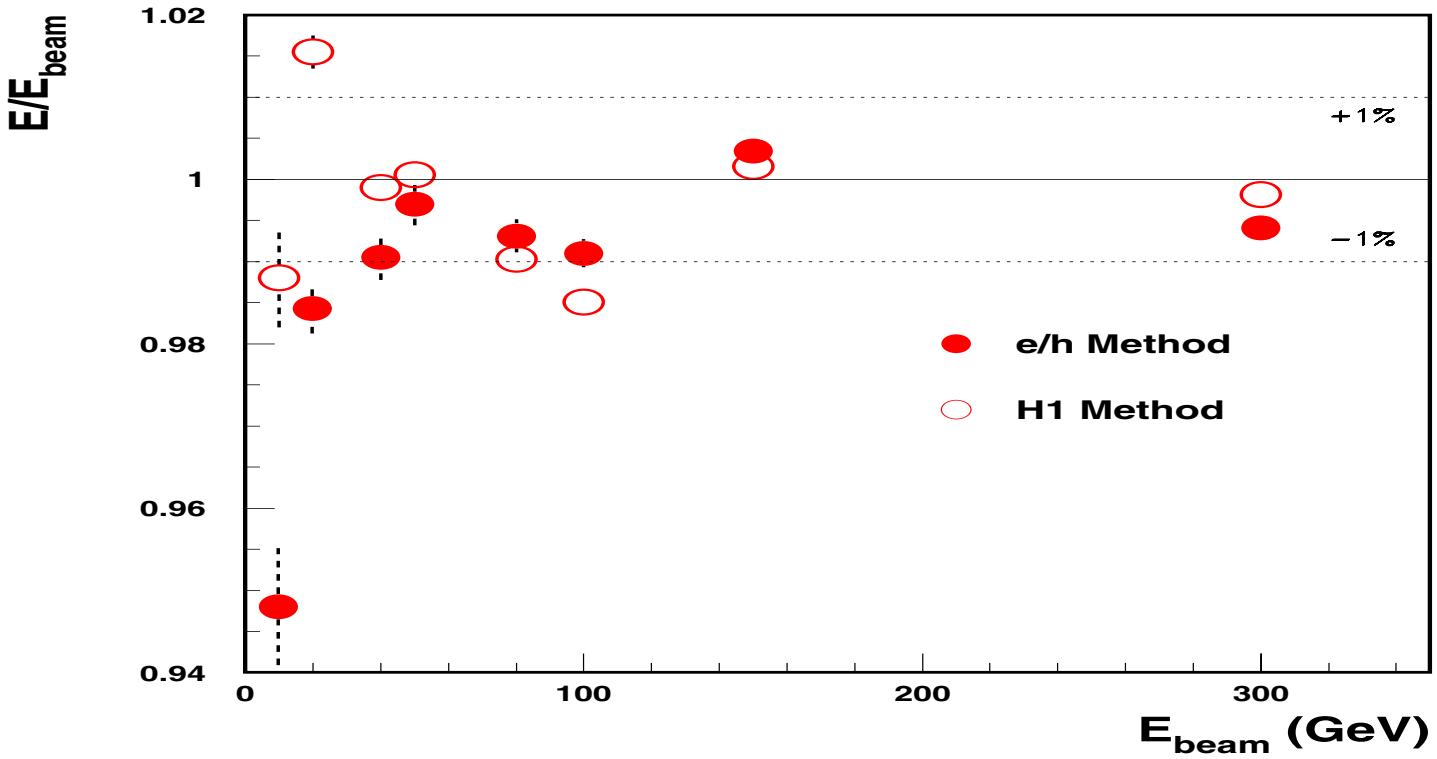

Figure 10: Energy linearity as a function of the beam energy for the e/h method (black circles) and the cells weighting method (open circles).

Linearity: e/h and BM

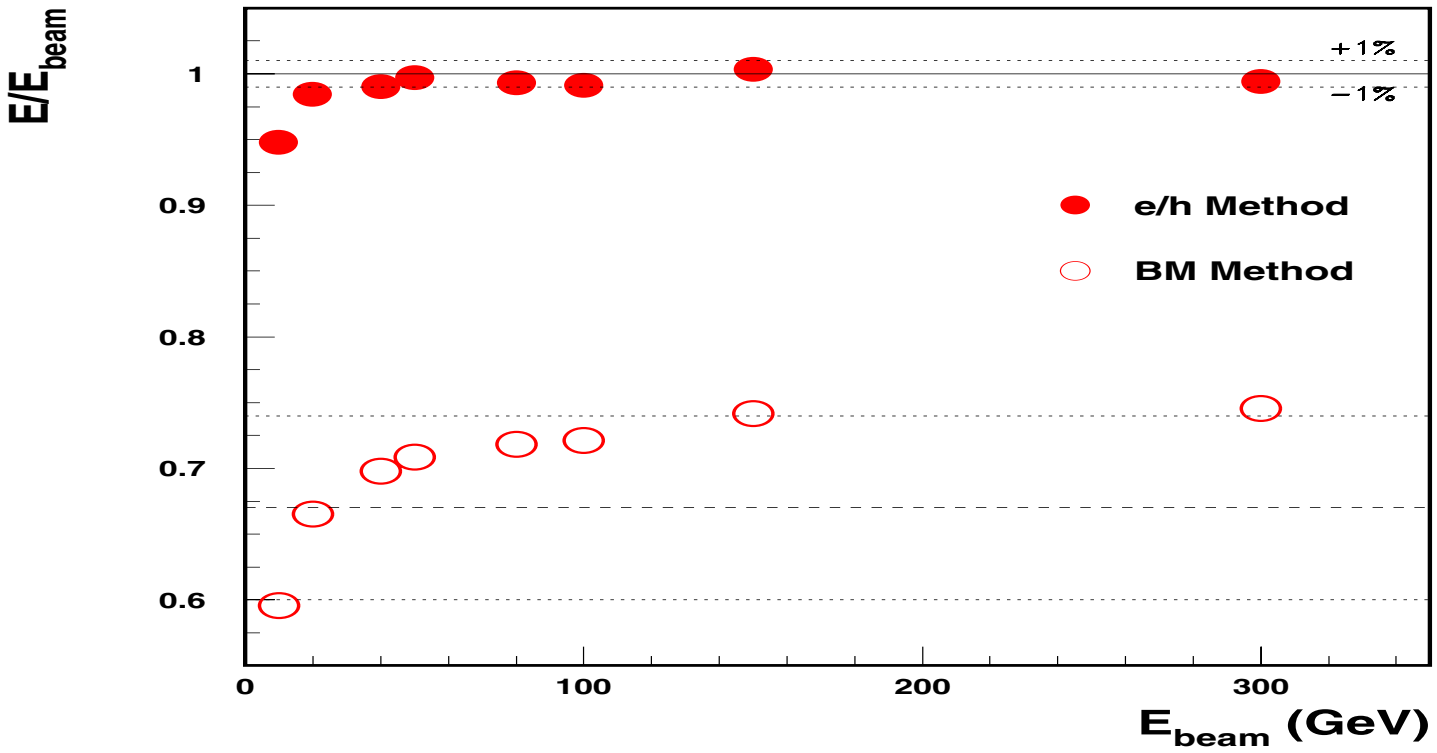

Figure 11: Energy linearity as a function of the beam energy for the e/h method (black circles) and the benchmark method (open circles).


Energy Resolutions

Figure 12 shows the fractional energy resolutions (σ/E) as a function of $1/\sqrt{E_{beam}}$ obtained by three methods: the e/h method (black circles), the benchmark method (crosses), and the cells weighting method (open circles). As can be seen, the energy resolutions for the e/h method are comparable with the benchmark method and only of 30% worse than for the cells weighting method. A fit to the data points gives the fractional energy resolution for the e/h method obtained using the iteration procedure with $\epsilon = 0.1\%$:

$$\frac{\sigma}{E} = \left[\frac{(58 \pm 3)\%\sqrt{GeV}}{\sqrt{E}} + (2.5 \pm 0.3)\%\right] \oplus \frac{(1.7 \pm 0.2)\ GeV}{E} \ .$$

Resolution

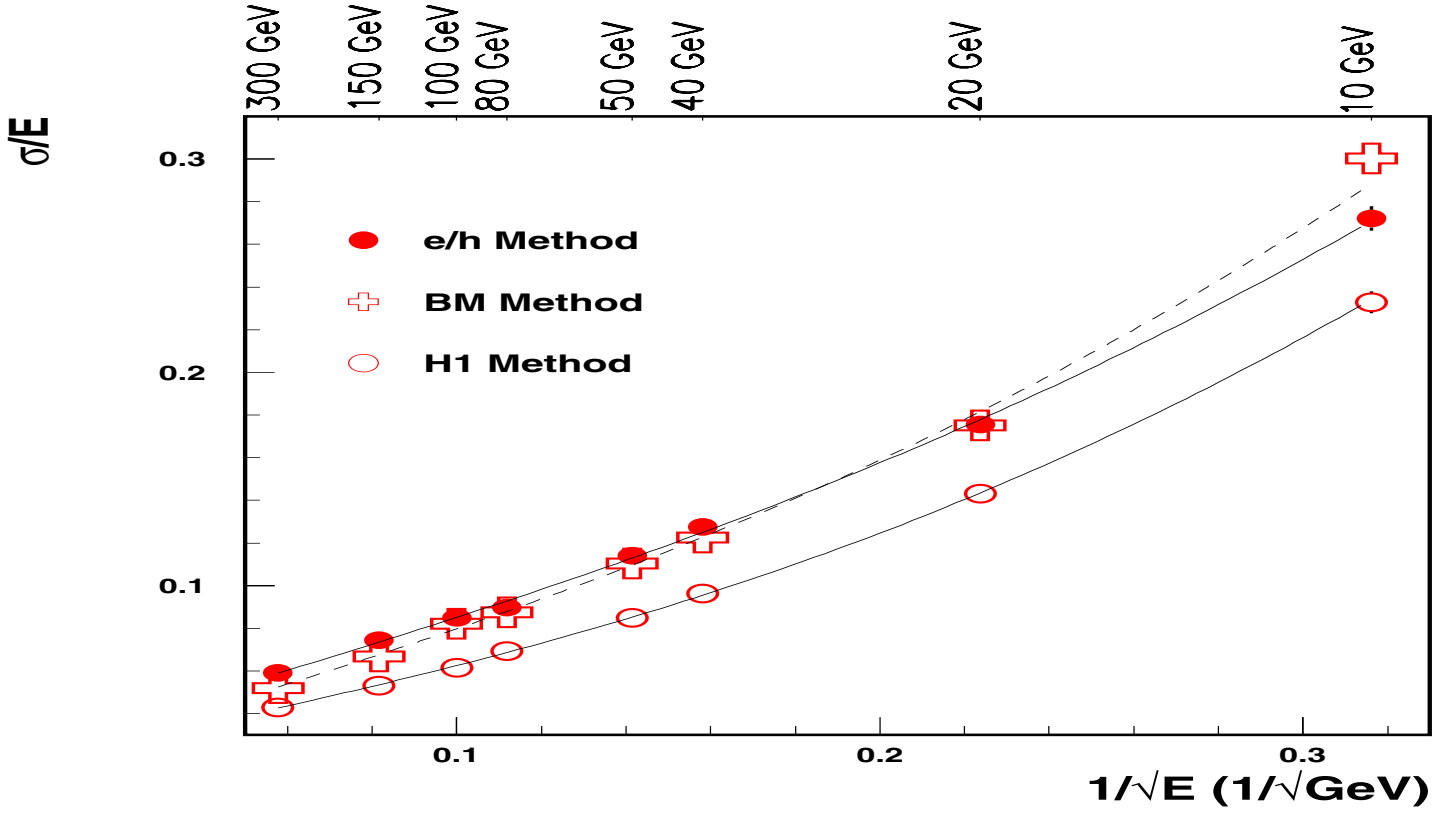

Figure 12: The energy resolutions obtained with the e/h method (black circles), the benchmark method (crosses) and the cells weighting method (circles).


Energy Resolutions *(continued)*

For the e/h method using the first approximation:

$$\frac{\sigma}{E} = \left[\frac{(56 \pm 3)\%\sqrt{GeV}}{\sqrt{E}} + (2.7 \pm 0.3)\%\right] \oplus \frac{(1.8 \pm 0.2)\ GeV}{E} \ .$$

For the benchmark method:

$$\frac{\sigma}{E} = \left[\frac{(60 \pm 3)\%\sqrt{GeV}}{\sqrt{E}} + (1.8 \pm 0.2)\%\right] \oplus \frac{(2.0 \pm 0.1)\ GeV}{E} \ .$$

For the cells weighting method:

$$\frac{\sigma}{E} = \left[\frac{(42 \pm 2)\%\sqrt{GeV}}{\sqrt{E}} + (1.8 \pm 0.1)\%\right] \oplus \frac{(1.8 \pm 0.1)\ GeV}{E} \ .$$


Hadronic Shower Development

We used this energy reconstruction method and obtained the energy depositions, E_i, in each longitudinal sampling with the thickness of Δx_i in units λ_π. Figure 13 shows the differential energy depositions

$$(\Delta E/\Delta x)_i = E_i/\Delta x_i$$

as a function of the longitudinal coordinate x for 10 – 300 GeV.

Longitudinal Profiles

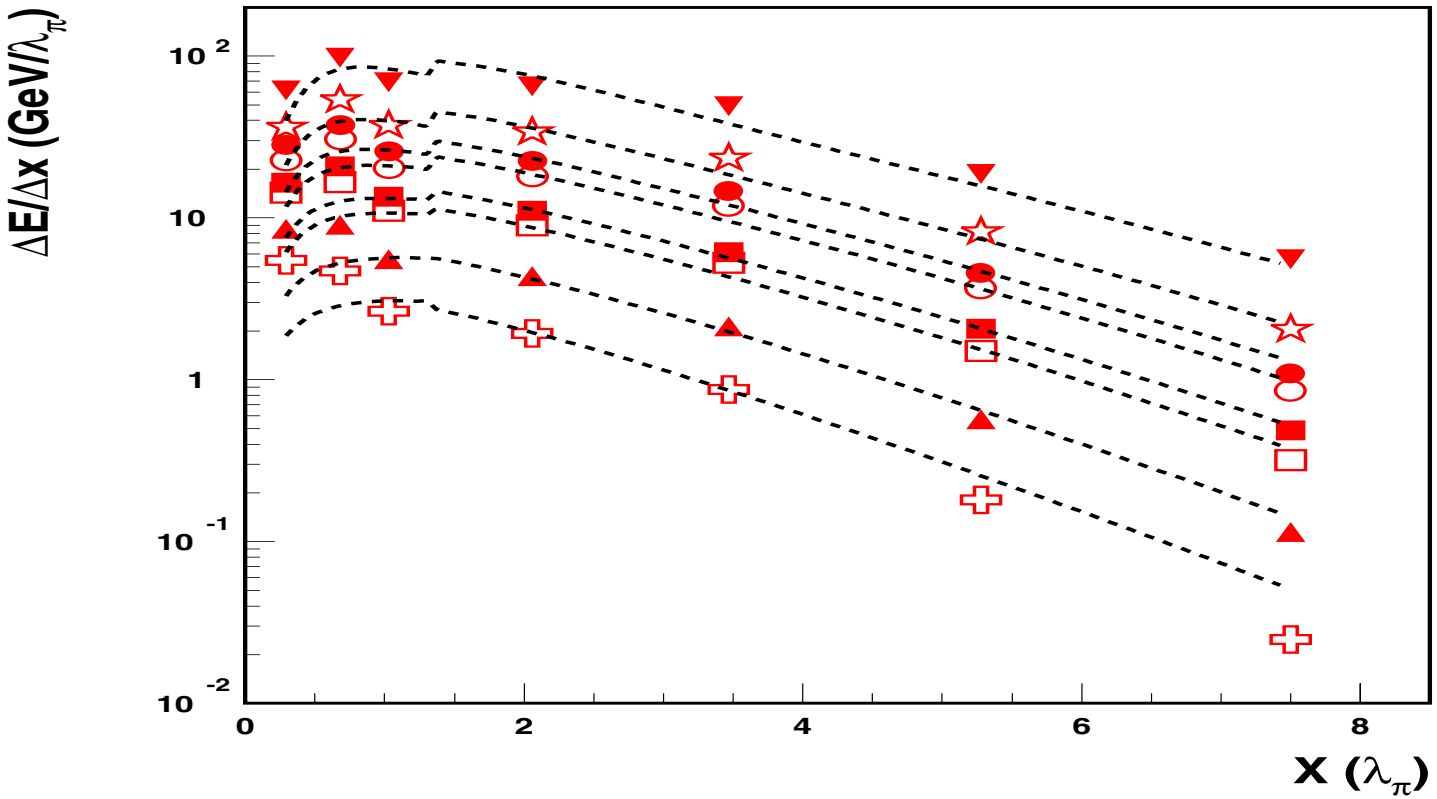

Figure 13: The longitudinal energy depositions at 10, 20, 40, 50, 80, 100, 150 and 300 GeV.

Longitudinal Parameterization

There is the well known parameterization of the longitudinal hadronic shower development from the shower origin

$$\frac{dE_s(x)}{dx} = N\left\{w\left(\frac{x}{X_0}\right)^{a-1} e^{-b\frac{x}{X_0}} + (1-w)\left(\frac{x}{\lambda_I}\right)^{a-1} e^{-d\frac{x}{\lambda_I}}\right\}, \quad (11)$$

where X_0 is the radiation length, λ_I is the interaction length, N is the normalization factor and parameters: $a = 0.6165 + 0.3193\ lnE$, $b = 0.2198$, $d = 0.9099 - 0.0237\ lnE$, $\omega = 0.4634$.


Shower Parameterization

We used the analytical representation of the hadronic shower longitudinal development from the calorimeter face:

$$\frac{dE(x)}{dx} = N\left\{\frac{wX_0}{a}\left(\frac{x}{X_0}\right)^a e^{-b\frac{x}{X_0}}\,{}_1F_1\left(1, a+1, \left(b-\frac{X_0}{\lambda_I}\right)\frac{x}{X_0}\right)\right.$$
$$\left. +\frac{(1-w)\lambda_I}{a}\left(\frac{x}{\lambda_I}\right)^a e^{-d\frac{x}{\lambda_I}}\,{}_1F_1\left(1, a+1, (d-1)\frac{x}{\lambda_I}\right)\right\} \quad (12)$$

here ${}_1F_1(\alpha, \beta, z)$ is the confluent hypergeometric function. The values of X_0, λ_I and the e/h ratios are different for electromagnetic and hadronic compartments of a combined calorimeter. So, it is impossible straightforward use of the formula (12) for the description of a combined calorimetry.


Shower Parameterization *(continued)*

We suggested the following algorithm of combination of the electromagnetic calorimeter (em) and hadronic calorimeter (had) curves of the differential longitudinal energy deposition dE/dx. At first, a hadronic shower develops in the electromagnetic calorimeter to the boundary value x_{em} which corresponds to certain integrated measured energy $E_{em}(x_{em})$. Then, using the corresponding integrated hadronic curve, $E(x) = \int_0^x (dE/dx)dx$, the point x_{had} is found from equation

$$E_{had}(x_{had}) = E_{em}(x_{em}) + E_{dm} \ .$$

From this point a shower continues to develop in the hadronic calorimeter.


Shower Parameterization *(continued)*

Figure 14 shows the differential energy depositions $(\Delta E/\Delta x)_i = E_i/\Delta x_i$ as a function of the longitudinal coordinate x in units λ_π for the 10 – 300 GeV and comparison with the combined curves for the longitudinal hadronic shower profiles (the dashed lines). It can be seen that there is a significant disagreement between the experimental data and the combined curves in the region of the LAr calorimeter and especially at low energies.

Longitudinal Profiles

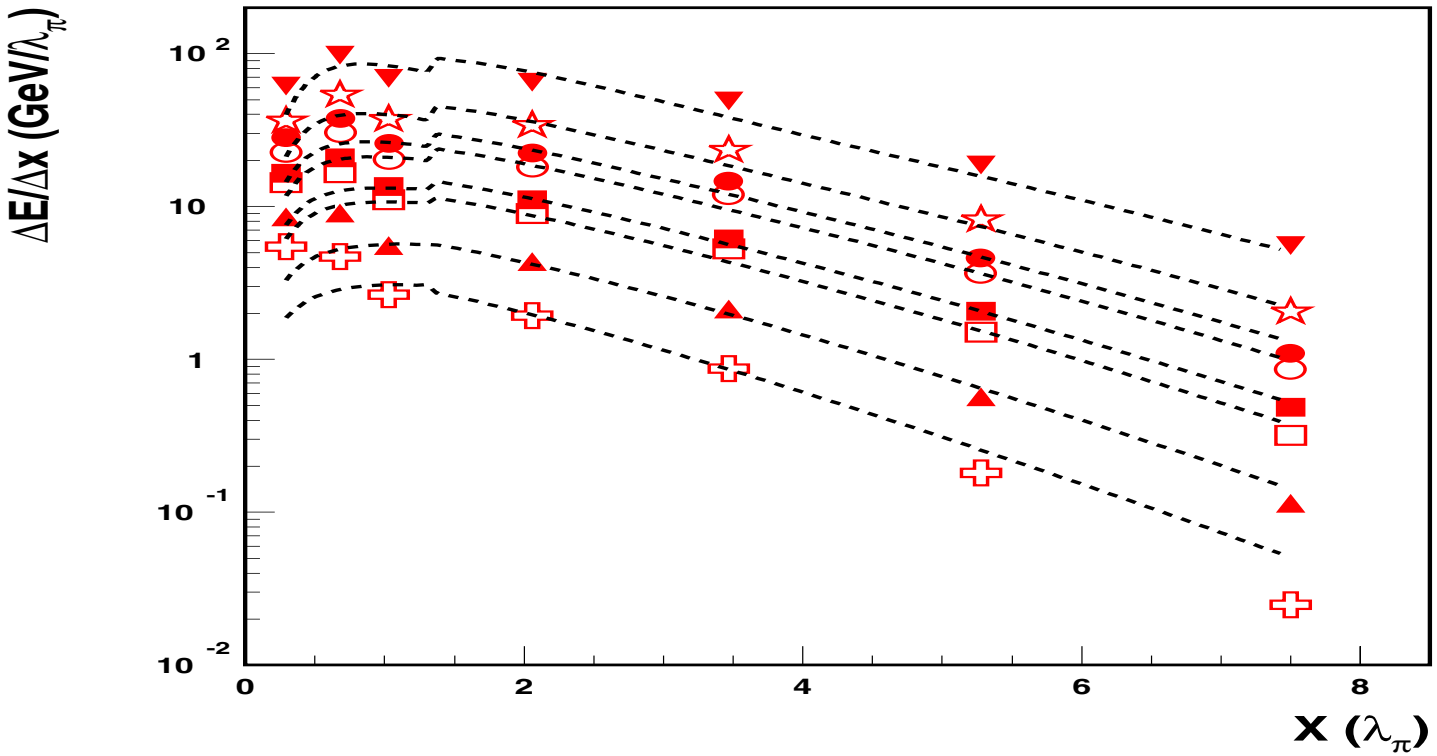

Figure 14: The longitudinal energy depositions at 10, 20, 40, 50, 80, 100, 150 and 300 GeV and the results of the description by the Bock (dashed lines).


Modification of Shower Parameterization

We attempted to improve the description and to include such essential feature of a calorimeter as the e/h ratio. Several modifications and adjustments of some parameters of this parameterization have been tried. It turned out that the changes of two parameters b and w in the formula (12) in such a way that

$$b = 0.22 \cdot (e/h)_{cal}/(e/h)'_{cal} \ , \quad w = 0.6 \cdot (e/\pi)_{cal}/(e/\pi)'_{cal}$$

made it possible to obtain the reasonable description of the experimental data. Here the values of the $(e/h)'_{cal}$ ratios are $(e/h)'_{em} \approx 1.1$ and $(e/h)'_{had} \approx 1.3$ which correspond to the data used for the Bock et al. parameterization. The $(e/\pi)'_{cal}$ are calculated using formula (3).


Modification *(continued)*

In Figure 15 the experimental differential longitudinal energy depositions and the results of the description by the modified parameterization (the solid lines) are compared. There is a reasonable agreement (probability of description is more than 5%) between the experimental data and the curves taking into account uncertainties in the parametrization function. In such case the Bock et al. parameterization is the private case for some fixed the e/h ratio.

Longitudinal Profiles

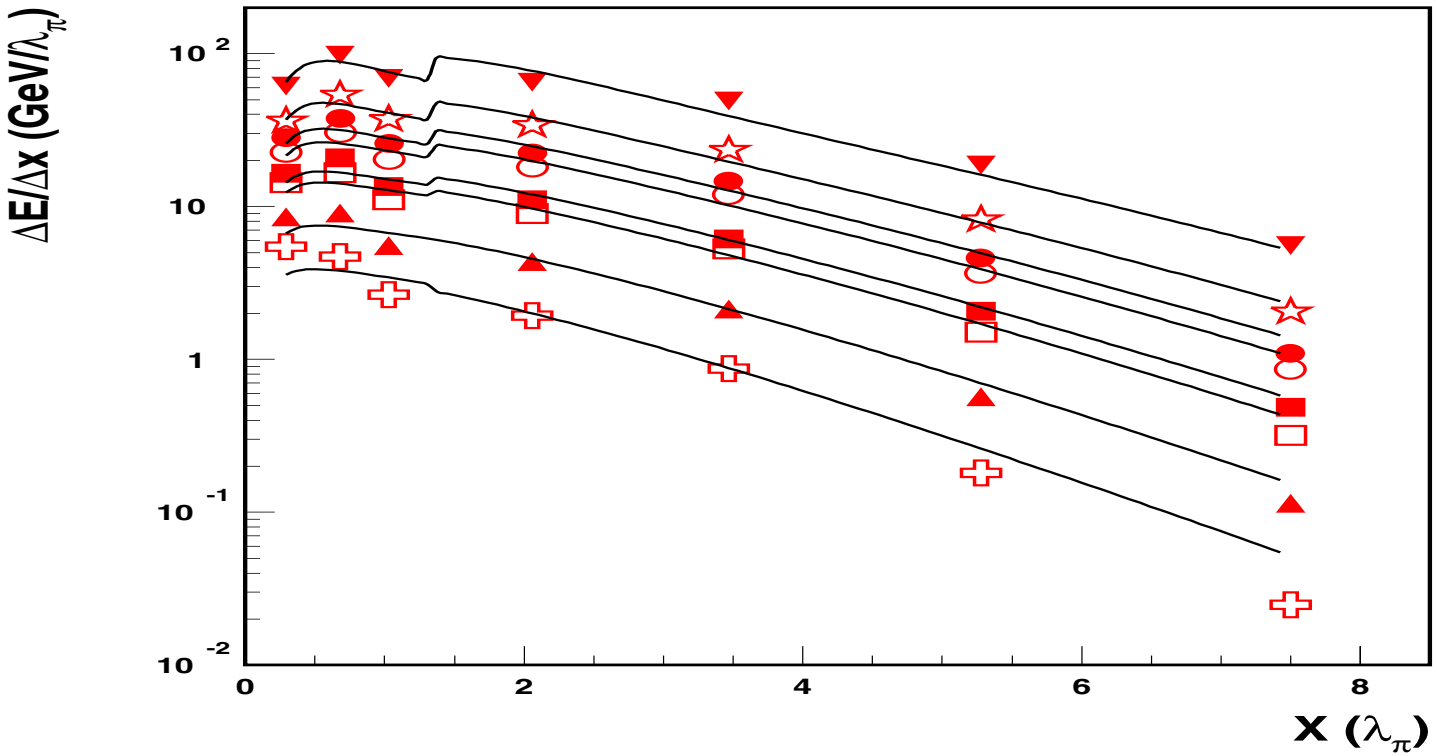

Figure 15: The longitudinal energy depositions at 10, 20, 40, 50, 80, 100, 150 and 300 GeV and the results of the description by the modified (solid lines) parameterizations.


Energy Deposition in Compartments

The obtained parameterization has some additional applications. For example, this formula may be used for an estimate of the energy deposition in various parts of a combined calorimeter. This demonstrates in Figure 16 in which the measured and calculated relative values of the energy deposition in the LAr and Tile calorimeters are presented. The relative energy deposition in the LAr calorimeter decreases from about 50% at 10 GeV to 30% at 300 GeV. On the contrary, the one in Tile calorimeter increases with the energy increasing.

Energy Depositions

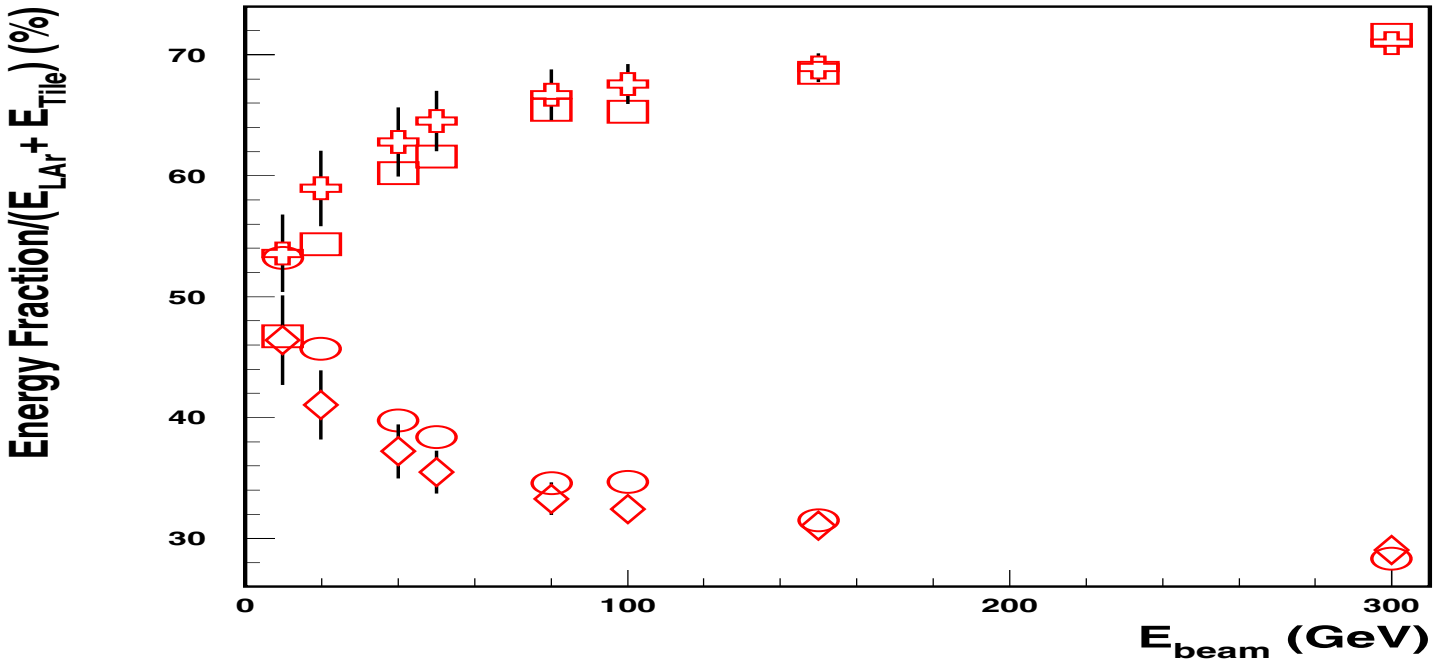

Figure 16: Energy depositions in the LAr and Tile versus E_{beam}. The circles (squares) are the measured energy in the LAr (Tile) calorimeter, the diamonds (crosses) are the calculated energy in the ones.


Conclusions

Hadron energy reconstruction for the ATLAS barrel prototype combined calorimeter, consisting of the lead-liquid argon electromagnetic part and the iron-scintillator hadronic part, in the framework of the non-parametrical method has been fulfilled.

The non-parametrical method of the energy reconstruction for a combined calorimeter uses only the known e/h ratios and the electron calibration constants, does not require the determination of any parameters by a minimization technique and can be used for the fast energy reconstruction in the first level trigger. The correctness of the reconstruction of the mean values of energies within $\pm 1\%$ has been demonstrated. The obtained fractional energy resolution is

$$[(58 \pm 3)\%/\sqrt{E} + (2.5 \pm 0.3)\%] \oplus (1.7 \pm 0.2)/E \ .$$


Conclusions

The obtained value of the e/h ratio for electromagnetic compartment of the combined calorimeter is 1.74 ± 0.04 and agrees with the prediction that $e/h > 1.7$ for this electromagnetic calorimeter.

The results of the study of the longitudinal hadronic shower development are presented.